Temporal Alterations in the Secretome of the Selective Ligninolytic Fungus *Ceriporiopsis subvermispora* during Growth on Aspen Wood Reveal This Organism's Strategy for Degrading Lignocellulose

Chiaki Hori,[a,b] Jill Gaskell,[a] Kiyohiko Igarashi,[b] Phil Kersten,[a] Michael Mozuch,[a] Masahiro Samejima,[b] Dan Cullen[a]

U.S. Department of Agriculture, Forest Products Laboratory, Madison, Wisconsin, USA[a]; Department of Biomaterials Sciences, Graduate School of Agricultural and Life Sciences, University of Tokyo, Tokyo, Japan[b]

The white-rot basidiomycetes efficiently degrade all wood cell wall polymers. Generally, these fungi simultaneously degrade cellulose and lignin, but certain organisms, such as *Ceriporiopsis subvermispora*, selectively remove lignin in advance of cellulose degradation. However, relatively little is known about the mechanism of selective ligninolysis. To address this issue, *C. subvermispora* was grown in liquid medium containing ball-milled aspen, and nano-liquid chromatography-tandem mass spectrometry was used to identify and estimate extracellular protein abundance over time. Several manganese peroxidases and an aryl alcohol oxidase, both associated with lignin degradation, were identified after 3 days of incubation. A glycoside hydrolase (GH) family 51 arabinofuranosidase was also identified after 3 days but then successively decreased in later samples. Several enzymes related to cellulose and xylan degradation, such as GH10 endoxylanase, GH5_5 endoglucanase, and GH7 cellobiohydrolase, were detected after 5 days. Peptides corresponding to potential cellulose-degrading enzymes GH12, GH45, lytic polysaccharide monooxygenase, and cellobiose dehydrogenase were most abundant after 7 days. This sequential production of enzymes provides a mechanism consistent with selective ligninolysis by *C. subvermispora*.

The white-rot basidiomycetes are efficient degraders of plant cell walls, the most abundant terrestrial carbon source. The origin of these fungi was coincident with the sharp decrease in the rate of organic carbon burial (1), implying that they have played a crucial role in the global carbon cycle. Recent emphasis on "biorefinery," conversions of plant resources into high-value, low-molecular-weight compounds has increased interest in the unique bioprocesses of these fungi.

It is well established that the white-rot basidiomycetes can be distinguished by their decay patterns (1–6). One group includes the model ligninolytic fungus *Phanerochaete chrysosporium*, which degrades cellulose, hemicellulose, and lignin simultaneously. Another group, exemplified by *Ceriporiopsis subvermispora*, can selectively remove lignin in advance of cellulose degradation. Mechanisms of selective ligninolysis remain uncertain, although the genetics and physiology of white-rot fungi have advanced considerably in recent years.

The extracellular oxidative enzymes lignin peroxidase (LiP), manganese peroxidase (MnP), versatile peroxidase (VP), and laccase have been implicated in lignin degradation. Among these, class II peroxidases such as LiP and MnP are able to depolymerize synthetic lignin *in vitro* (7–9). Complete systems require peroxide, which may be generated by pyranose oxidase (10), methanol oxidase (11), aryl alcohol oxidase (AAO) (12), and the copper radical oxidase glyoxal oxidase (GLOX) (13). These redox enzymes were recently categorized as auxiliary activity (AA) families (14).

Degradation of cellulose and hemicellulose in plant cell walls typically involves an array of glycoside hydrolases (GHs) broadly categorized as cellulases and hemicellulases. On the basis of amino acid sequence, these enzymes can be classified into carbohydrate-active enzyme (CAZyme) families in the CAZy database (http://www.cazy.org) (15). Members of certain families may be functionally uniform, e.g., GH6 "exo" cellobiohydrolases, while others exhibit substantial heterogeneity, e.g., GH5 hemicellulases or cellulases.

C. subvermispora secretes several isoenzymes of MnP and laccase (16, 17) but not LiPs (18). The oxidation potential of MnPs is insufficient to cleave the major nonphenolic linkages in lignin, but the reaction may be mediated by lipid peroxidation (19). Recent analysis of the *C. subvermispora* genome confirmed the expression of MnP and laccase genes (20). LiP-like genes were also identified, but expression levels were negligible in media containing ball-milled aspen (BMA) as the sole carbon source. Relative to untreated wood, accessibility of this pulverized forestry feedstock is substantially increased, thereby permitting rapid growth of a wide range of wood decay fungi (5, 20). Under these conditions, transcriptome and secretome analysis of *C. subvermispora* suggested that higher expression of oxidoreductases and lower expression of CAZymes relative to *P. chrysosporium* might explain selective ligninolysis (20).

Nevertheless, the definitive mechanism(s) underlying selective degradation remain unsettled. Mass spectrometry-based secretome analysis provided an inventory of soluble extracellular proteins but was limited to a single time point (20). To further understanding of the process, secretome profiles were determined at different times using nano-liquid chromatography-tandem mass

spectrometry (nano-LC-MS/MS). In addition, we conducted transcriptome sequencing (RNA-seq) analysis of *C. subvermispora* grown in the liquid medium containing BMA.

MATERIALS AND METHODS

Fungal strain and culture conditions. *Ceriporiopsis subvermispora* strain B, the sequenced monokaryotic isolate (21), was obtained from the U.S. Department of Agriculture Forest Mycology Center (Madison, WI) and maintained on potato dextrose agar plates at room temperature (26.5°C). Mycelial plugs were used to inoculate 250 ml of Highley's basal salt medium (22) containing 0.5% (wt/vol) ball-milled bigtooth aspen (*Populus grandidentata*) as a sole carbon source. The basal medium contained, per liter, 2 g of NH_4NO_3, 2 g of KH_2PO_4, 0.5 g of $MgSO_4 \cdot 7H_2O$, 0.1 g of $CaCl_2 \cdot 2H_2O$, 1 mg of thiamine hydrochloride, and 10 ml of mineral solution. Mineral solution contained, per liter, 1.5 g of nitrilotriacetic acid, 3 g of $MgSO_4 \cdot 7H_2O$, 0.5 g of $MnSO_4 \cdot H_2O$, 1 g of NaCl, 0.1 g of $FeSO_4 \cdot H_2O$, 0.1 g of $CoSO_4$, 0.1 g of $CaCl_2$, 0.1 g of $ZnSO_4 \cdot 7H_2O$, 0.01 g of $CuSO_4$, 0.01 g of $AlK(SO_4)_2 \cdot 12H_2O$, 0.01 g of H_3BO_3, and 0.01 g of $NaMoO_4 \cdot 2H_2O$. The 2-liter Erlenmeyer flasks were incubated on a rotary shaker (150 rpm) at room temperature for 3, 5, or 7 days. For enzyme assays and mass spectroscopic analysis, culture filtrates were separated from mycelia and insoluble substrate by filtration through Miracloth (CN Biosciences, La Jolla, CA) and stored at −20°C. For RNA analysis, mycelia were harvested after 5 days and immediately frozen at −80°C. For enzyme assays, three replicate cultures were harvested at each time point.

Assay of oxidoreductases related to degradation of lignocellulose. The protein concentration of culture filtrates was determined by the Bradford assay (Sigma-Aldrich, Buchs, Switzerland) according to the manufacturer's instructions. Measurement of manganese peroxidase activity was based on the oxidative dimerization of 2,6-dimethoxyphenol (2,6-DMP). The reaction mixture contained 100 μM 2,6-DMP, 100 μM $MnSO_4$, 50 mM sodium tartrate (pH 4.5), 50 μM H_2O_2, and culture filtrate in 1,000 μl. Oxidation was monitored at 477 nm, and the molar extinction coefficient (ε_{477}) was 14,800 M^{-1} cm^{-1}. Lignin peroxidase activity was determined by conversion of veratryl alcohol (Sigma-Aldrich) into veratraldehyde in the presence of H_2O_2 (23). A 50 mM concentration of sodium tartrate (pH 3.0) served as a buffer, and the culture filtrate was mixed with 2 mM veratryl alcohol and 0.4 mM H_2O_2 in 1,000 μl at room temperature. The reaction was monitored at 310 nm, and activity was calculated using an ε_{310} of 9,256 M^{-1} cm^{-1} for veratraldehyde. Laccase activity was assayed with 2,2-azonodi-3-ethylbenzothiazoline-6-sulfuric acid (ABTS; Boehringer, Mannheim, Germany) as a substrate in 30 mM glycine-HCl buffer (pH 3.0) at room temperature. The reaction mixture contained 14 μM ABTS and culture filtrate in 1,000 μl. The reaction was monitored at 436 nm, and an ε_{436} of 29,300 M^{-1} cm^{-1} was used for the product. Aryl alcohol activity was estimated spectrophotometrically by oxidation of 5 mM 4-methoxybenzyl alcohol (Sigma-Aldrich) to the corresponding aldehyde (ε_{285} = 16,950 M^{-1} cm^{-1}) in 100 mM potassium phosphate buffer (pH 6.0). For cellobiose dehydrogenase (CDH) activity, cytochrome *c* reduction was assayed using cellobiose as a substrate as described previously (24).

Protein identification by nano-LC-MS/MS. As described previously (1, 5, 6), soluble proteins of culture filtrates on days 3, 5, and 7 were precipitated by direct addition of solid trichloroacetic acid to 10% (wt/vol). After tryptic digestion, the generated peptides were subjected to nano-liquid chromatography separation using an Agilent 1100 nanoflow system (Agilent, Palo Alto, CA). The chromatography system was coupled to a hybrid linear ion trap-Orbitrap mass spectrometer (LTQ-Orbitrap; Thermo Fisher Scientific, San Jose, CA) equipped with a nano electrospray ion source as described previously (25, 26). The acquired MS/MS spectra were analyzed by in-house-licensed Mascot search engine (Matrix Science, London, United Kingdom) using annotated gene models from the *C. subvermispora*, version 1.0, genome database (http://genome.jgi-psf.org/Cersu1/Cersu1.home.html).

Mascot searches were performed with the following parameters: a fragment ion mass tolerance of 0.6 Da, a parent ion tolerance of 15 ppm, and methionine oxidation as a variable modification. Scaffold software (version Scaffold_3_00_6; Proteome Software Inc., Portland, OR) was used to validate MS/MS-based peptide and protein identifications. Protein identifications were accepted if they contained at least 2 uniquely identified peptides and if protein probabilities exceeded 95.0%, as determined by the Protein Prophet algorithm (27). Detailed information for each identified proteins was accessed via the Joint Genome Institute's (JGI) Genome Portal (28), including Gene Ontology, InterPro domain, and blastp search results. For certain genes, the deduced amino acid sequences were manually rechecked by blastp search of the NCBI database. Function or "putative" function was assigned when it was supported by direct experimental evidence or when comparisons to known proteins revealed conserved catalytic features and/or significant alignment scores (bit scores of 150) to known proteins. In the case of CAZymes, glycoside hydrolase (GH) family 5 members were subdivided into subfamilies as described previously (29), but in the absence of direct experimental support, all activities should be considered tentative. All other proteins were designated "hypothetical." Approximate protein abundance in each of the cultures was expressed as the number of unique peptides and the exponentially modified protein abundance index (emPAI) value (30). The emPAI values of all 248 proteins were normalized and hierarchically clustered based on protein expression patterns using GeneSpring, version 12.

RNA sequence-based expression analysis. Total RNA was purified from frozen mycelium as described previously (31). The Illumina TruSeq protocol was used to prepare samples for Illumina Genome Analyzer IIx (GAIIx) sequencing. Briefly, a NanoDrop spectrophotometer and Agilent 2100 BioAnalyzer were used to verify RNA purity and integrity, respectively. Each RNA-seq library was generated using Illumina's *TruSeq RNA Sample Preparation Guide* (32) and the Illumina TruSeq RNA sample preparation kit (Illumina Inc., San Diego, CA). mRNA was purified from 1 μg of total RNA using poly(T) oligonucleotide-attached magnetic beads. Double-stranded cDNAs were synthesized using SuperScript II (Invitrogen, Carlsbad, CA) and random primers for first-strand cDNA synthesis followed by second-strand synthesis using DNA polymerase I and RNase H for removal of mRNA. Double-stranded cDNA was purified using Agencourt AMPure XP beads (Qiagen, Valencia, CA) as recommended in the *TruSeq RNA Sample Preparation Guide*. cDNAs were end repaired by T4 DNA polymerase and Klenow DNA polymerase and phosphorylated by T4 polynucleotide kinase. The blunt-ended cDNA was purified using Agencourt AMPure XP beads. The cDNA products were incubated with Klenow DNA polymerase to add an A base to the 3′ end of the blunt phosphorylated DNA fragments and then purified using Agencourt AMPure XP beads. DNA fragments are ligated to Illumina adapters, which have a single T base overhang at their 3′ end. The adapter-ligated products were purified using Agencourt AMPure XP beads. Adapter-ligated DNAs were amplified in a linker-mediated PCR (LM-PCR) for 15 cycles using Phusion DNA polymerase and Illumina's PE genomic DNA primer set and then purified using Agencourt AMPure XP beads. Images were analyzed using CASAVA, version 1.8.2, and FASTQ files deposited with NCBI Sequence Read Archive (study accession number SRP032796). DNAStar Inc. (Madison, WI) modules SeqNGen and Qseq were used for mapping the unpaired 36-bp reads and for statistical analysis. Microarray analysis was previously published (20), and the data are available under Gene Expression Omnibus (GEO) accession number GSE34636.

RESULTS

Over the course of 7 days, soluble proteins increased (1.39 ± 0.42 mg liter^{-1}, 1.86 ± 0.32 mg liter^{-1}, and 2.88 ± 0.59 mg liter^{-1} on days 3, 5, and 7, respectively) and nano-LC-MS/MS

FIG 1 Distribution of *C. subvermispora* proteins identified by LC-MS/MS in media containing BMA on days 3, 5, and 7 (A) and the aggregate number of proteins within AA and CAZy families identified during cultivation (B). "Other" proteins are largely without recognizable secretion signals and likely intracellular proteins released by hyphal lysis during incubation. Low-molecular-weight proteins, those without accessible trypsin cleavage sites, those bound to the lignocellulose substrate, and rapidly degraded proteins are likely to be underestimated or missed entirely by shotgun LC-MS/MS.

revealed shifting expression profiles. A total of 243, 204, and 133 proteins were unambiguously identified in the culture filtrates on day 3, 5, and 7, respectively, and these were assigned to broad functional categories (Fig. 1A; see also supplemental material). The proportion of carbohydrate-active enzymes (CAZymes) related to cellulose and hemicellulose degradation, such as glycoside hydrolases (GHs) and carbohydrate esterases (CEs), increased from 31% to 43% over the same period. Most of this increase was due to GHs (27% to 38%). Auxiliary activities (AAs) potentially associated with lignin degradation such as manganese peroxidases and some oxidases moderately rose,

from 11% to 13% of the detected proteins. Likewise, peptidases and lipases showed modest increases, from 12% to 14% and from 4% to 5%, respectively. In contrast, the percentage of "other" proteins decreased from 26% to 10% and hypothetical proteins decreased slightly, from 17% to 16%. Thus, as cultivation time advanced, the number of the detectable proteins decreased, while the proportion of CAZymes and AAs associated with cell wall degradation increased. Detailed annotation of detected AA and CAZy proteins revealed considerable functional diversity (Fig. 1B).

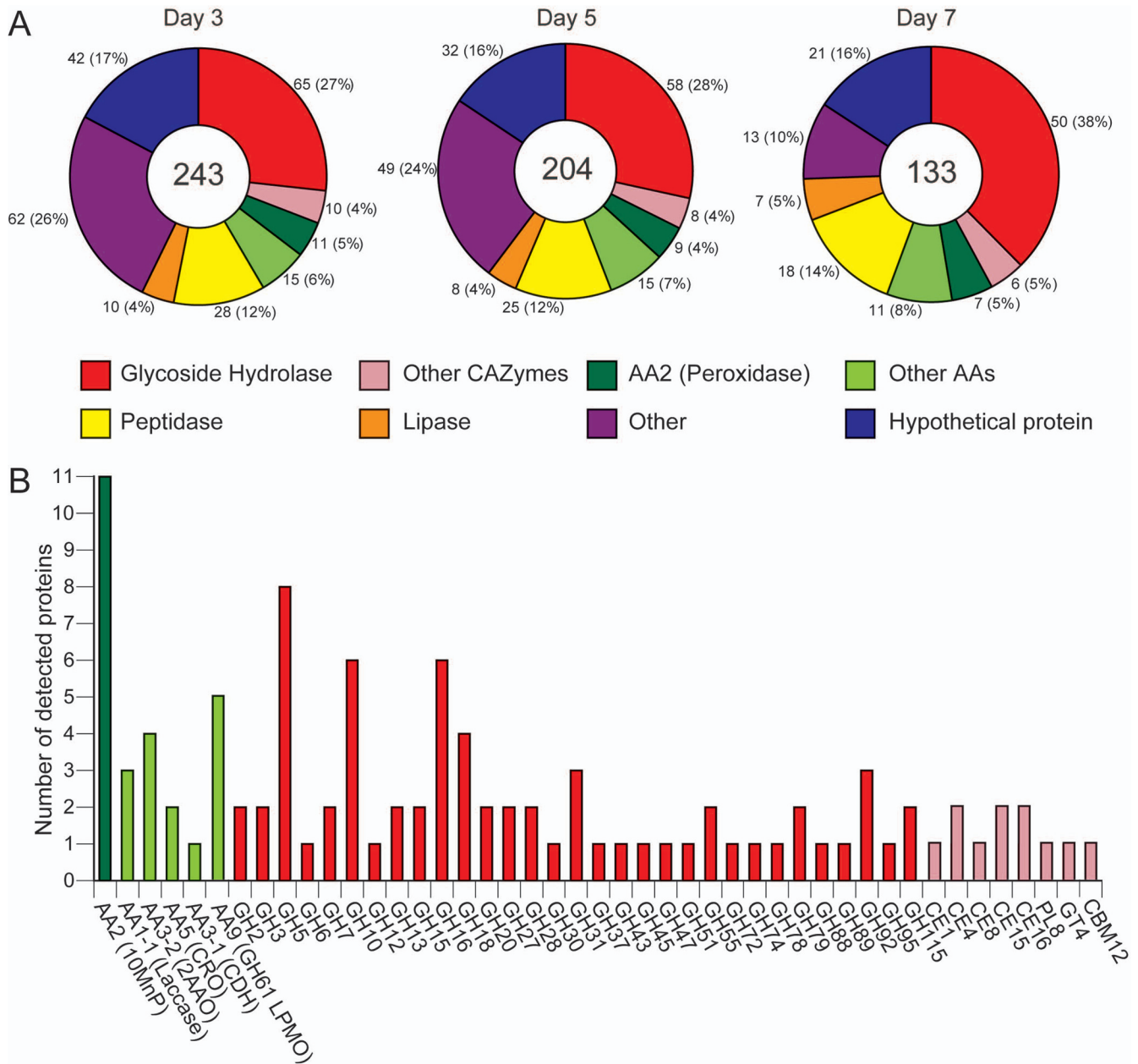Protein abundance was approximated by emPAI values and

TABLE 1 Ten most abundant proteins expressed by *C. subvermispora* during growth in media containing aspen wood on days 3, 5, and 7 by using LC-MS/MS

Day	ID[a]	Putative function	Peptide[b]	emPAI[c]
3	50297	Peroxidase MnP	7	63.78
	118681	Peptidase A1	8	29.61
	78979	Hypothetical	3	24.00
	50686	Peroxidase MnP	7	20.42
	117240	Peptidase A1	8	7.31
	162360	GH51 arabinofuranosidase	11	6.93
	84544	Aryl alcohol oxidase	13	4.76
	94398	Peroxidase MnP	4	4.50
	49863	Peroxidase MnP	7	4.44
	86951	Lipase	12	4.20
5	50297	Peroxidase MnP	8	94.48
	79557	GH5_5 endoglucanase-CBM1	4	35.75
	97858	GH10 endoxylanase-CBM1	12	18.94
	78979	Hypothetical	3	10.25
	115988	Peptidase A1	8	6.42
	21396	CE15 glucuronoyl esterase	8	6.15
	59733	GH10 endoxylanase-CBM1	11	5.47
	89943	GH7 exocellobiohydrolase-CBM1	8	5.26
	117240	Peptidase A1	9	5.23
	86951	Lipase	12	5.03
7	97858	GH10 endoxylanase-CBM1	13	62.01
	89943	GH7 exocellobiohydrolase-CBM1	8	31.82
	79557	GH5_5 endoglucanase-CBM1	4	23.34
	115988	Peptidase A1	9	19.68
	50297	Peroxidase MnP	6	13.37
	111819	GH12 endoglucanase	3	13.10
	136606	GH7 exocellobiohydrolase-CBM1	9	11.61
	85474	AA9/GH61 polysaccharide monooxygenase	4	11.13
	21396	CE15 glucuronoyl esterase	8	9.64
	82023	GH45 endoglucanse V-like	3	6.70

[a] For protein identification (ID), detailed information is available via the JGI genome website (http://genome.jgi.doe.gov/Cersu1/Cersu1.home.html).
[b] Unique peptide counts identified by LC-MS/MS.
[c] emPAI is described in Materials and Methods.

ranked on this basis. The 10 most abundant proteins included four manganese peroxidases (MnPs), an aryl alcohol oxidase (AAO), a GH51 arabinofuranosidase (Araf), two peptidases, and a lipase on day 3 (Table 1). On day 5, MnP (50297) remained the most abundant protein, whereas a GH5_5 endoglucanase (EG) and a GH10 endoxylanase (EX) were also easily detected. Other CAZys included a CE15 glucuronoyl esterase (Gle) and a GH7 cellobiohydrolase (CBH), likely involved in xylan and cellulose degradation, respectively. On day 7, the GH10 EX (97858) displaced MnP as the most abundant protein. In addition to GH5_5 EG and GH7 CBHs, GH12 EG, GH45 EG, and GH61 lytic polysaccharide monooxygenase (LPMO; recently designated AA9) appeared as abundant proteins, suggesting that the diversity of highly expressed cellulases may increase over time.

Temporal expression patterns were examined more closely (Fig. 2). Certain AA families, including MnPs and an AAO (117387), decreased overall. Other GMC oxidoreductases, laccases, and copper radical oxidases (CRO2) remained unchanged or, in the case of laccase protein 84170, increased. Cellobiose dehydrogenase (CDH) and LPMOs, oxidative enzymes thought to be involved in cellulose degradation, increased as well. Proteins classified as GH families 5, 6, 7, 10, 12, 45, and 51 and CE families 1 and 15 also increase, but GH51 Araf (162360) showed the opposite trend. In the case of GH5s, increases were observed for GH5_5 EGs (79557 and 117046) and for GH5_7 endomannanase (94795).

To visualize overall expression patterns, including hypothetical proteins, emPAI values of 248 detected proteins were normalized and hierarchically clustered based on gene expression patterns (Fig. 3A). Among 248 proteins, 34 proteins exhibited significant changes over time and were categorized into 6 clusters (Fig. 3B). Clusters 1, 2, and 3, mainly comprised of CAZymes, showed increasing trends. In contrast, clusters 4, 5, and 6 contained decreasing levels of MnPs and AAO. Possibly playing an important role in lignocellulose degradation, hypothetical proteins were assigned to clusters 1, 4, and 6. Interestingly, certain peptidases were coexpressed with cellulases and peroxidases.

To affirm LC-MS/MS results, MnP, lignin peroxidase (LiP), laccase, AAO, glyoxal oxidase (GLOX), and CDH activities were assayed in culture filtrates (Fig. 4). Consistent with secretome analysis, activities for MnP, laccase, and AAO, but not LiP or GLOX, were detected during cultivation. In addition, CDH activity was relatively stable on days 3 and 5 but then increased significantly on day 7. This result was consistent with the time course of CDH based on emPAI values (Fig. 2). In contrast to the abovementioned enzymes, all CDH activity is attributable to a single-copy gene.

We examined the relationship between protein abundance and transcript levels determined by previously published microarrays (20) and by RNA-seq. A total of 6,082 genes exhibiting RPKM values (reads per kilobase per million mapped reads) of >10 had also been measured by microarrays, and these were, as expected, positively correlated ($r = 0.431$; $n = 6,082$). Using the nine most highly regulated genes (BMA/Glc >10-fold) as examples, the relationships between transcript levels, regulation, and emPAI values are presented in Table 2. At least one RNA-seq read was mapped to a total of 10,820 genes, and their expression ranged from $\log_2$ RPKM values of -6.59 to 14.19 (see supplemental material). For aspen-expressed genes showing significant transcript accumulation by microarray, the RNA-seq $\log_2$ RPKM values ranged from 4.41 to 12.68, further supporting their high expression in 5-day-old cultures. Of 21,145,137 filtered reads, 17,361,555 (82%) mapped to predicted transcripts. Gene models corresponding to the secreted proteins were examined closely, and no evidence of incorrect models and/or alternative splicing was observed.

DISCUSSION

Ceriporiopsis subvermispora efficiently degrades plant cell walls, and decay is characterized by selective ligninolysis. Much is known about the MnPs and laccases, although polysaccharide degradation has received relatively little attention (33). In the present study, secretome analysis provided a broad view of cell wall degradation.

When *C. subvermispora* was cultivated in the media containing the complex lignocellulose substrate BMA, production of extracellular proteins increased and the pattern of detectable proteins changed over time. CAZymes and AAs related to degradation of lignocellulose were clearly induced (Fig. 1A).
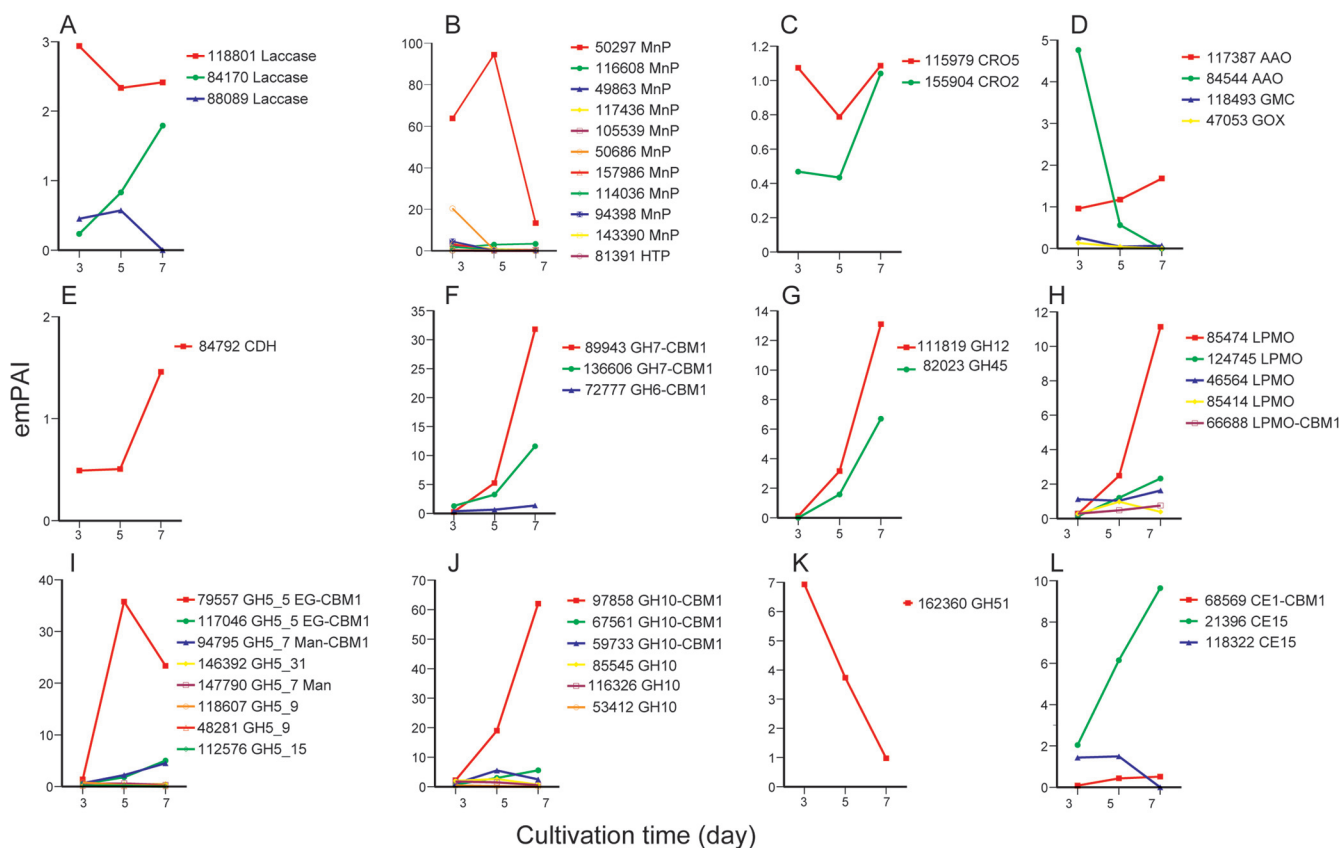
FIG 2 Time course of emPAI values of enzymes associated with lignocellulose degradation secreted by *C. subvermispora* grown in media containing BMA. (A) AA1; (B) AA2; (C) AA5; (D) AA3-2; (E) AA3-1; (F) GH6 and GH7; (G) GH12 and GH45; (H) AA9/GH61; (I) GH5; (J) GH10; (K) GH51; (L) CE1 and CE15.

Ten MnPs and three laccases were identified (Fig. 1B), and several MnPs were highly expressed as early as day 3 (Table 1). Most MnPs decreased over time (Fig. 2), and LiP- or VP-like peroxidases (20) were not detected at any point. In the case of oxidases, which might supply peroxide to the class II peroxidases, two AAOs and two copper radical oxidases were detected (Fig. 1B). Only one AAO (117387) decreased over time, paralleling MnPs (Fig. 3B and 4). AAO has been identified in several white-rot fungi, including another selective lignin degrader, *Pleurotus eryngii* (34, 35). This white-rot fungus also secretes manganese peroxidase, versatile peroxidase, and laccase along with AAO, but it, too, produces no lignin peroxidase (20). These results suggested that *C. subvermispora* utilized a system of lignin degradation similar to that of *P. eryngii*.

Such genetic repertoires and expression patterns differ substantially from those of *P. chrysosporium*, which possesses no laccase-encoding genes but secretes LiP, MnP, and GLOX in nutrient-starved media (36). Unlike for *C. subvermispora*, these oxidative enzymes have not been detected in media containing BMA, even after extended incubation (5).

In contrast to the ligninolytic system, polysaccharide degradation by *C. subvermispora* employs many secreted enzymes in common with *P. chrysosporium*. For degradation of cellulose, both species secrete GH7 CBH1, GH6 CBH2, GH5_5 EGs, GH12 EGs, and EG GH45 (37). In addition to hydrolases, oxidoreductases such as LPMO (AA9/GH61) and CDH are gener-

ally thought to be involved in cellulose degradation (38–41). In this study, all of these enzymes were detected (Fig. 1B) and their levels increased sharply over time, except for EG GH5_5 (Fig. 2). CDH activity in the culture filtrates was increased along with emPAI values (Fig. 4).

Previous secretome analysis of *P. chrysosporium* showed that GH10 and GH11 endoxylanases (EXs), GH51 arabinofuranosidase (Araf), CE1 acetyl/feruroyl esterase, and CE15 glucuronoyl esterase (Gle) probably contributed to xylan degradation (5, 31, 37, 42–44). Among these, only GH11 EX was undetectable during *C. subvermispora* cultivation (Fig. 1B), and this has been noted for other white-rot members of Polyporales (1, 45). In contrast to these other GHs, GH51 Araf was most abundant on day 3 (Fig. 2). In addition to well-characterized proteins, many hypothetical proteins were secreted and, in aggregate, represented 16 to 17% of total detected proteins (Fig. 1A). Based on hierarchical clustering, three hypothetical proteins (112878, 87564, and 78979) showed an expression pattern very similar to that of CAZymes or AAs, with increasing or decreasing trends, respectively (Fig. 3B). Likewise, peptidases were 12 to 14% of total detected proteins (Fig. 1A). The appearance of peptidases 115988 and 118681 seemed coordinate with cellulases and peroxidases, respectively (Fig. 3B). In *P. chrysosporium*, proteases were thought to be involved in activating or inactivating cellulases and peroxidases (25, 46). The *C. subvermispora* proteases might also play important roles in cycling the limited nitrogen in wood. Later sampling might provide in-
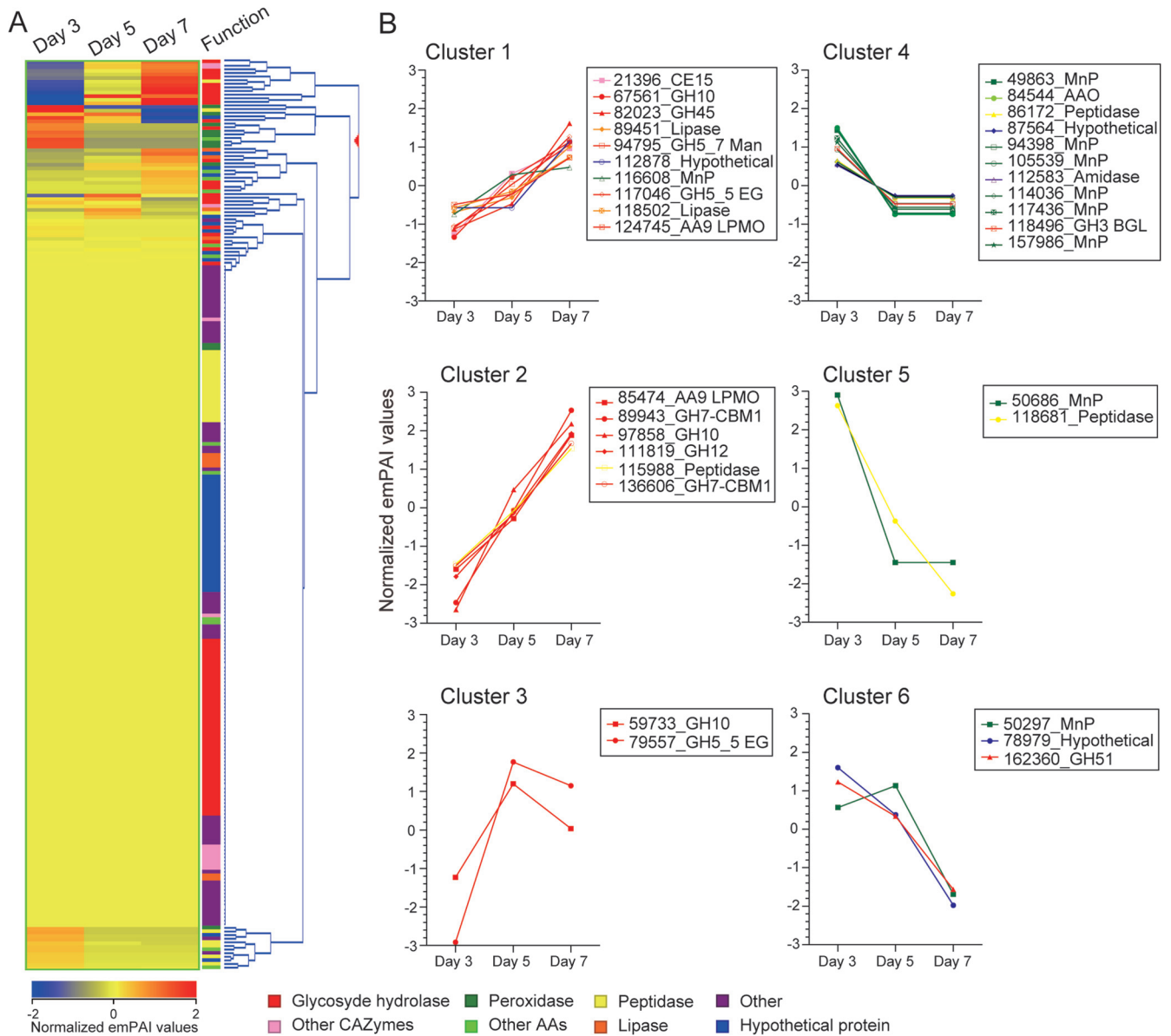
FIG 3 (A) Hierarchical analysis of protein expression patterns of 248 detected genes based on normalized emPAI values. (B) Thirty-four genes with significant changes were categorized into six clusters.

sight along these lines, although autolysis becomes problematic in older BMA cultures (5).

The shifting detection of proteins may reflect the unique patterns of *C. subvermispora* ligninolysis. At early stages of cultivation, four MnPs and AAO were mainly expressed, which reasonably accounts for active lignin removal in advance of cellulose degradation. Interestingly, GH51 Araf was also secreted on day 3 with lignin-degrading enzymes. In wood, arabinose is a minor component and mainly replaced with glucuronoxylan (47). In grass, substituted arabinose is attached with ferulic acid ester, which could be cross-linked with lignin to prevent enzymatic saccharification (26). Although there is no evidence that ferulate exists in wood, production of GH51 Araf at early stages may support efficient lignin removal of *C. subvermispora*. By day 5, GH10 EX, GH5_5 EG, and GH7 CBH, acting on main

chains of xylan and/or cellulose, followed. Finally, GH10 EX became a dominant protein, along with a variety of cellulose-degrading enzymes such as GH5_5 EG, GH7 CBH, GH12 EG, GH45 EG, and AA9/GH61 LPMO.

LPMO was recently reported to degrade cellulose chains by oxidative mechanisms (34, 39, 41). In addition, CDH has been purported to be involved in cellulose degradation, participating with GH7 and/or LPMO (34, 40, 45). Indeed, production of CDH increased (Fig. 2), as well as GH7 cellobiohydrolase and LPMO. These enzymes are also secreted by *P. chrysosporium* in cultures containing ball-milled pine (*Pinus strobus*) and, to a lesser extent, in BMA (5). In either case, it should be emphasized that these patterns do not mimic "natural" solid-wood decay, a process involving relatively slow colonization and often accompanied by a
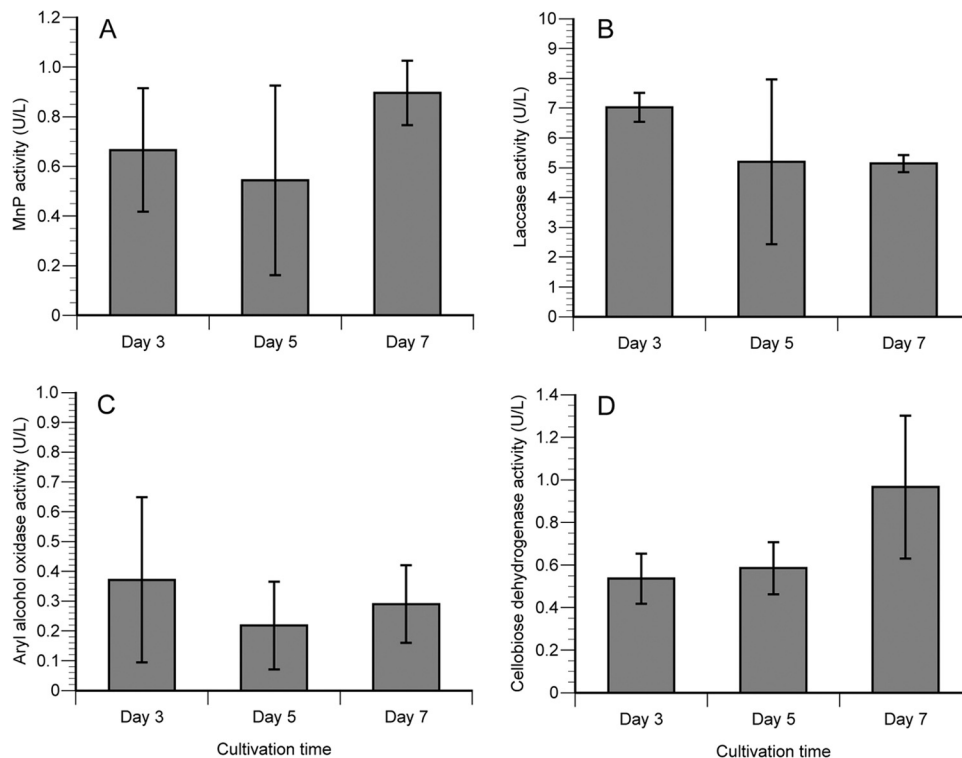
FIG 4 Manganese peroxidase (A), laccase (B), aryl alcohol oxidase (C), and cellobiose dehydrogenase (D) activities of culture filtrates produced by *C. subvermispora* grown in BMA cultures. Error bars indicate standard deviations from three replicate cultivations. Consistent with LC-MS/MS analysis, no LiP or GLOX activity was detected.

consortium of fungi and bacteria. The pulverized and submerged wood used in this study is highly accessible to enzymes, and simple carbohydrates are immediately available (5).

Nevertheless, the present work provides strong biological evidence for sequential degradation by *C. subvermispora*, albeit under a narrow set of conditions: linkages within lignin and between lignin and hemicellulose are attacked early by ligninolytic enzymes and possibly GH51, followed by cleavage of hemicellulose and cellulose main chains by endo-acting enzymes and, finally, by cellulose degradation involving oxidative and hydrolytic reactions

TABLE 2 Transcripts with >10-fold accumulation determined by microarrays after 5 days of growth in BMA cultures relative to glucose culture, RNA-seq-based transcript levels (RPKM), and the LC-MS/MS expression pattern of the corresponding proteins during growth in BMA cultures

		Microarrays[a]			RNA-seq RPKM (log$_2$)	Mass spectrometry					
						Unique peptides			emPAI		
ID[b]	Putative function	Glc (log$_2$)	BMA (log$_2$)	BMA/Glc		Day 3	Day 5	Day 7	Day 3	Day 5	Day 7
66688	Polysaccharide monooxygenase (AA9/GH61)-CBM1	9.62	14.87	37.9	5.19	2	2	2	0.28	0.48	0.75
94795	Endoglucanase (GH5_5)-CBM1	9.54	14.35	28.05	10.44	3	5	5	0.65	2.20	4.51
46564	Polysaccharide monooxygenase (AA9/GH61)	10.35	14.94	24.07	5.63	3	3	3	1.12	1.04	1.62
85414	Polysaccharide monooxygenase (AA9/GH61)	9.59	14.14	23.52	7.21	1	2	1	0.26	0.97	0.38
84792	Cellobiose dehydrogenase	9.29	13.76	22.24	4.41	7	8	11	0.49	0.51	1.46
59733	Endoxylanase (GH10)-CBM1	9.24	13.69	21.78	9.31	6	11	9	1.01	5.47	2.44
79557	Endoglucanase (GH5_5)-CBM1	10.24	14.04	13.87	12.68	4	4	4	1.39	35.75	23.34
87580	Carbohydrate acetylesterase (CE16)-CBM1	10.94	14.46	11.54	6.58	0	2	3	0.00	0.24	0.86
67561	Endoxylanase (GH10)-CBM1	10.3	13.71	10.64	5.57	4	6	7	0.75	2.94	5.56

[a] Previously described by Fernandez-Fueyo et al. (20) and listed under GEO accession number GSE34636.
[b] For protein identification (ID), detailed information is available via the JGI genome website (http://genome.jgi.doe.gov/Cersu1/Cersu1.home.html).

by a variety of enzymes. This sequential enzyme secretion may be in response to the challenging ultrastructure of plant cell walls, in which cellulose fibrils are surrounded by hemicellulose and lignin (48). Further support of this view will require biochemical analyses of specific enzymes (e.g., Araf) as well as microscopic localization of the enzymes in relation to cell wall decay over time.

ACKNOWLEDGMENTS

REFERENCES

1. **Floudas D, Binder M, Riley R, Barry K, Blanchette RA, Henrissat B, Martinez AT, Otillar R, Spatafora JW, Yadav JS, Aerts A, Benoit I, Boyd A, Carlson A, Copeland A, Coutinho PM, de Vries RP, Ferreira P, Findley K, Foster B, Gaskell J, Glotzer D, Gorecki P, Heitman J, Hesse C, Hori C, Igarashi K, Jurgens JA, Kallen N, Kersten P, Kohler A, Kues U, Kumar TK, Kuo A, LaButti K, Larrondo LF, Lindquist E, Ling A, Lombard V, Lucas S, Lundell T, Martin R, McLaughlin DJ, Morgenstern I, Morin E, Murat C, Nagy LG, Nolan M, Ohm RA, Patyshakuliyeva A, Rokas A, Ruiz-Duenas FJ, Sabat G, Salamov A, et al.** 2012. The Paleozoic origin of enzymatic lignin decomposition reconstructed from 31 fungal genomes. Science **336**:1715–1719. http://dx.doi.org/10.1126/science.1221748.

2. **Blanchette R.** 1991. Delignification by wood-decay fungi. Annu. Rev. Phytopathol. **29**:381–398. http://dx.doi.org/10.1146/annurev.py.29.090191.002121.

3. **Blanchette RA, Burnes TA, Eerdmans MM, Akhtar M.** 1992. Evaluating isolates of *Phanerochaete chrysosporium* and *Ceriporiopsis subvermispora* for use in biological pulping processes. Holzforschung **46**:109–115. http://dx.doi.org/10.1515/hfsg.1992.46.2.109.

4. **Otjen L, Blanchette R, Effland M, Leatham G.** 1987. Assessment of 30 white rot basidiomycetes for selective lignin degradation. Holzforschung **41**:343–349. http://dx.doi.org/10.1515/hfsg.1987.41.6.343.

5. **Vanden Wymelenberg A, Gaskell J, Mozuch M, BonDurant SS, Sabat G, Ralph J, Skyba O, Mansfield SD, Blanchette RA, Grigoriev IV, Kersten PJ, Cullen D.** 2011. Significant alteration of gene expression in wood decay fungi *Postia placenta* and *Phanerochaete chrysosporium* by plant species. Appl. Environ. Microbiol. **77**:4499–4507. http://dx.doi.org/10.1128/AEM.00508-11.

6. **Vanden Wymelenberg A, Gaskell J, Mozuch MD, Sabat G, Ralph J, Skyba O, Mansfield S, Blanchette RA, Martinez D, Grigoriev I, Kersten P, Cullen D.** 2010. Comparative transcriptome and secretome analysis of wood decay fungi *Postia placenta* and *Phanerochaete chrysosporium*. Appl. Environ. Microbiol. **76**:3599–3610. http://dx.doi.org/10.1128/AEM.00058-10.

7. **Hammel K, Jensen K, Mozuch M, Landucci L, Tien M, Pease E.** 1993. Ligninolysis by a purified lignin peroxidase. J. Biol. Chem. **268**:12274–12281.

8. **Hammel KE, Moen MA.** 1991. Depolymerization of a synthetic lignin *in vitro* by lignin peroxidase. Enzyme Microb. Technol. **13**:15–18. http://dx.doi.org/10.1016/0141-0229(91)90182-A.

9. **Wariishi H, Valli K, Gold MH.** 1991. *In vitro* depolymerization of lignin by manganese peroxidase of *Phanerochaete chrysosporium*. Biochem. Biophys. Res. Commun. **176**:269–275. http://dx.doi.org/10.1016/0006-291X(91)90919-X.

10. **Daniel G, Volc J, Kubatova E.** 1994. Pyranose oxidase, a major source of H_2O_2 during wood degradation by *Phanerochaete chrysosporium*, *Trametes versicolor*, and *Oudemansiella mucida*. Appl. Environ. Microbiol. **60**:2524–2532.

11. **Nishida A, Eriksson KE.** 1987. Formation, purification and partial characterization of methanol oxidase, a H_2O_2-producing enzyme in *Phanerchaete chrysosporium*. Biotechnol. Appl. Biochem. **9**:325–338.

12. **Guillén F, Martinez AT, Martinez MJ.** 1992. Substrate specificity and properties of the aryl-alcohol oxidase from the ligninolytic fungus *Pleurotus eryngii*. Eur. J. Biochem. **209**:603–611. http://dx.doi.org/10.1111/j.1432-1033.1992.tb17326.x.

13. **Kersten PJ, Kirk TK.** 1987. Involvement of a new enzyme, glyoxal oxidase, in extracellular H_2O_2 production by *Phanerochaete chrysosporium*. J. Bacteriol. **169**:2195–2201.

14. **Levasseur A, Drula E, Lombard V, Coutinho PM, Henrissat B.** 2013. Expansion of the enzymatic repertoire of the CAZy database to integrate auxiliary redox enzymes. Biotechnol. Biofuels **6**:41. http://dx.doi.org/10.1186/1754-6834-6-41.

15. **Lombard V, Golaconda Ramulu H, Drula E, Coutinho PM, Henrissat B.** 2014. The carbohydrate-active enzymes database (CAZy) in 2013. Nucleic Acids Res. **42**:D490–D495. http://dx.doi.org/10.1093/nar/gkt1178.

16. **Lobos S, Larrain J, Salas L, Cullen D, Vicuna R.** 1994. Isozymes of manganese-dependent peroxidase and laccase produced by the lignin-degrading basidiomycete *Ceriporiopsis subvermispora*. Microbiology **140**:2691–2698. http://dx.doi.org/10.1099/00221287-140-10-2691.

17. **Salas C, Lobos S, Larrain J, Salas L, Cullen D, Vicuna R.** 1995. Properties of laccase isoenzymes produced by the basidiomycete *Ceriporiopsis subvermispora*. Biotechnol. Appl. Biochem. **21**:323–333.

18. **Ruttimann C, Schwember E, Salas L, Cullen D, Vicuna R.** 1992. Ligninolytic enzymes of the white rot basidiomycetes *Phlebia brevispora* and *Ceriporiopsis subvermispora*. Biotechnol. Appl. Biochem. **16**:64–76.

19. **Bao W, Fukushima Y, Jensen KA, Moen MA, Hammel KE.** 1994. Oxidative degradation of non-phenolic lignin during lipid peroxidation by fungal manganese peroxidase. FEBS Lett. **354**:297–300. http://dx.doi.org/10.1016/0014-5793(94)01146-X.

20. **Fernandez-Fueyo E, Ruiz-Duenas FJ, Ferreira P, Floudas D, Hibbett DS, Canessa P, Larrondo LF, James TY, Seelenfreund D, Lobos S, Polanco R, Tello M, Honda Y, Watanabe T, Ryu JS, Kubicek CP, Schmoll M, Gaskell J, Hammel KE, St John FJ, Vanden Wymelenberg A, Sabat G, Splinter BonDurant S, Syed K, Yadav JS, Doddapaneni H, Subramanian V, Lavin JL, Oguiza JA, Perez G, Pisabarro AG, Ramirez L, Santoyo F, Master E, Coutinho PM, Henrissat B, Lombard V, Magnuson JK, Kues U, Hori C, Igarashi K, Samejima M, Held BW, Barry KW, LaButti KM, Lapidus A, Lindquist EA, Lucas SM, Riley R, Salamov AA, Hoffmeister D, Schwenk D, Hadar Y, Yarden O, et al.** 2012. Comparative genomics of *Ceriporiopsis subvermispora* and *Phanerochaete chrysosporium* provide insight into selective ligninolysis. Proc. Natl. Acad. Sci. U. S. A. **109**:5458–5463. http://dx.doi.org/10.1073/pnas.1119912109.

21. **Tello M, Seelenfreund D, Lobos S, Gaskell J, Cullen D, Vicuna R.** 2001. Isolation and characterization of homokaryotic strains from the ligninolytic basidiomycete *Ceriporiopsis subvermispora*. FEMS Microbiol. Lett. **199**:91–96. http://dx.doi.org/10.1111/j.1574-6968.2001.tb10656.x.

22. **Highley TL.** 1973. Influence of carbon source on cellulase activity of white rot and brown rot fungi. Wood Fiber **5**:50–58.

23. **Tien M, Kirk TK.** 1984. Lignin-degrading enzyme from *Phanerochaete chrysosporium*: purification, characterization, and catalytic properties of a unique H_2O_2-requiring oxygenase. Proc. Natl. Acad. Sci. U. S. A. **81**:2280–2284. http://dx.doi.org/10.1073/pnas.81.8.2280.

24. **Samejima M, Eriksson K-E.** 1992. A comparison of the catalytic properties of cellobiose:quinone oxidoreductase and cellobiose oxidase from *Phanerochaete chrysosporium*. Eur. J. Biochem. **207**:103–107. http://dx.doi.org/10.1111/j.1432-1033.1992.tb17026.x.

25. **Eriksson K-E, Pettersson B.** 1982. Purification and partial characterization of two acidic proteases from the white rot fungus *Sporotrichium pulverulentum*. Eur. J. Biochem. **124**:635–642.

26. **Scheller HV, Ulvskov P.** 2010. Hemicelluloses. Annu. Rev. Plant Biol. **61**:263–289. http://dx.doi.org/10.1146/annurev-arplant-042809-112315.

27. **Nesvizhskii AI, Keller A, Kolker E, Aebersold R.** 2003. A statistical model for identifying proteins by tandem mass spectrometry. Anal. Chem. **75**:4646–4658. http://dx.doi.org/10.1021/ac0341261.

28. **Grigoriev IV, Nordberg H, Shabalov I, Aerts A, Cantor M, Goodstein D, Kuo A, Minovitsky S, Nikitin R, Ohm RA, Otillar R, Poliakov A, Ratnere I, Riley R, Smirnova T, Rokhsar D, Dubchak I.** 2012. The genome portal of the Department of Energy Joint Genome Institute. Nucleic Acids Res. **40**:D26–D32. http://dx.doi.org/10.1093/nar/gkr947.

29. **Aspeborg H, Coutinho PM, Wang Y, Brumer H, Henrissat B.** 2012. Evolution, substrate specificity and subfamily classification of glycoside hydrolase family 5 (GH5). BMC Evol. Biol. **12**:186. http://dx.doi.org/10.1186/1471-2148-12-186.

30. **Ishihama Y, Oda Y, Tabata T, Sato T, Nagasu T, Rappsilber J, Mann M.** 2005. Exponentially modified protein abundance index (emPAI) for estimation of absolute protein amount in proteomics by the number of sequenced peptides per protein. Mol. Cell. Proteomics **4:**1265–1272. http://dx.doi.org/10.1074/mcp.M500061-MCP200.

31. **Vanden Wymelenberg A, Gaskell J, Mozuch MD, Kersten P, Sabat G, Martinez D, Cullen D.** 2009. Transcriptome and secretome analysis of *Phanerochaete chrysosporium* reveal complex patterns of gene expression. Appl. Environ. Microbiol. **75:**4058–4068. http://dx.doi.org/10.1128/AEM.00314-09.

32. **Illumina.** August 2011. TruSeq RNA sample preparation guide. Illumina part number 15008136, revision A. Illumina, San Diego, CA.

33. **Milagres AM, Magalhaes PO, Ferraz A.** 2005. Purification and properties of a xylanase from *Ceriporiopsis subvermispora* cultivated on *Pinus taeda*. FEMS Microbiol. Lett. **253:**267–272. http://dx.doi.org/10.1016/j.femsle.2005.09.055.

34. **Camarero S, Galletti GC, Martinez AT.** 1994. Preferential degradation of phenolic lignin units by two white rot fungi. Appl. Environ. Microbiol. **60:**4509–4516.

35. **Hernández-Ortega A, Ferreira P, Martinez AT.** 2012. Fungal aryl-alcohol oxidase: a peroxide-producing flavoenzyme involved in lignin degradation. Appl. Microbiol. Biotechnol. **93:**1395–1410. http://dx.doi.org/10.1007/s00253-011-3836-8.

36. **Vanden Wymelenberg A, Minges P, Sabat G, Martinez D, Aerts A, Salamov A, Grigoriev I, Shapiro H, Putnam N, Belinky P, Dosoretz C, Gaskell J, Kersten P, Cullen D.** 2006. Computational analysis of the *Phanerochaete chrysosporium* v2.0 genome database and mass spectrometry identification of peptides in ligninolytic cultures reveals complex mixtures of secreted proteins. Fungal Genet. Biol. **43:**343–356. http://dx.doi.org/10.1016/j.fgb.2006.01.003.

37. **Vanden Wymelenberg A, Sabat G, Martinez D, Rajangam AS, Teeri TT, Gaskell J, Kersten PJ, Cullen D.** 2005. The *Phanerochaete chrysosporium* secretome: database predictions and initial mass spectrometry peptide identifications in cellulose-grown medium. J. Biotechnol. **118:**17–34. http://dx.doi.org/10.1016/j.jbiotec.2005.03.010.

38. **Mansfield SD, deJong E, Saddler JN.** 1997. Cellobiose dehydrogenase, an active agent in cellulose depolymerization. Appl. Environ. Microbiol. **63:**3804–3809.

39. **Westereng B, Ishida T, Vaaje-Kolstad G, Wu M, Eijsink VG, Igarashi K, Samejima M, Stahlberg J, Horn SJ, Sandgren M.** 2011. The putative endoglucanase PcGH61D from *Phanerochaete chrysosporium* is a metal-dependent oxidative enzyme that cleaves cellulose. PLoS One **6:**e27807. http://dx.doi.org/10.1371/journal.pone.0027807.

40. **Langston JA, Shaghasi T, Abbate E, Xu F, Vlasenko E, Sweeney MD.** 2011. Oxidoreductive cellulose depolymerization by the enzymes cellobiose dehydrogenase and glycoside hydrolase 61. Appl. Environ. Microbiol. **77:**7007–7015. http://dx.doi.org/10.1128/AEM.05815-11.

41. **Harris PV, Welner D, McFarland KC, Re E, Navarro Poulsen JC, Brown K, Salbo R, Ding H, Vlasenko E, Merino S, Xu F, Cherry J, Larsen S, Lo Leggio L.** 2010. Stimulation of lignocellulosic biomass hydrolysis by proteins of glycoside hydrolase family 61: structure and function of a large, enigmatic family. Biochemistry **49:**3305–3316. http://dx.doi.org/10.1021/bi100009p.

42. **Adav SS, Ravindran A, Sze SK.** 2012. Quantitative proteomic analysis of lignocellulolytic enzymes by *Phanerochaete chrysosporium* on different lignocellulosic biomass. J. Proteomics **75:**1493–1504. http://dx.doi.org/10.1016/j.jprot.2011.11.020.

43. **Hori C, Igarashi K, Katayama A, Samejima M.** 2011. Effects of xylan and starch on secretome of the basidiomycete *Phanerochaete chrysosporium* grown on cellulose. FEMS Microbiol. Lett. **321:**14–23. http://dx.doi.org/10.1111/j.1574-6968.2011.02307.x.

44. **Sato S, Liu F, Koc H, Tien M.** 2007. Expression analysis of extracellular proteins from *Phanerochaete chrysosporium* grown on different liquid and solid substrates. Microbiology **153:**3023–3033. http://dx.doi.org/10.1099/mic.0.2006/000513-0.

45. **Hori C, Gaskell J, Igarashi K, Samejima M, Hibbett D, Henrissat B, Cullen D.** 2013. Genome-wide analysis of polysaccharide degrading enzymes in eleven white- and brown-rot polyporales provides insight into mechanisms of wood decay. Mycologia **105:**1412–1427. http://dx.doi.org/10.3852/13-072.

46. **Dosoretz CD, Chen H-C, Grethlein HE.** 1990. Effect of environmental conditions on extracellular protease activity in ligninolytic cultures of *Phanerochaete chrysosporium*. Appl. Environ. Microbiol. **56:**395–400.

47. **Timell T.** 1967. Recent progress in the chemistry of wood hemicelluloses. Wood Sci. Technol. **1:**45–70. http://dx.doi.org/10.1007/BF00592255.

48. **Ruel K, Chevalier-Billosta V, Guillemin F, Berrio-Sierra J, Joseleau JP.** 2006. The wood cell wall at the ultrastructural scale-formation and topochemical organization. Maderas Cien.Tecnol. **8:**107–116.